

## RESEARCH ARTICLE

# Solar PAR and UVR modify the community composition and photosynthetic activity of sea ice algae

Sara Enberg<sup>1,2,\*</sup>, Jonna Piiparinen<sup>1,3</sup>, Markus Majaneva<sup>1,2</sup>,  
Anssi V. Vähätalo<sup>4</sup>, Riitta Autio<sup>3</sup> and Janne-Markus Rintala<sup>1,2</sup>

<sup>1</sup>Tvärminne Zoological Station, University of Helsinki, J.A. Palménin tie 260, FI-10900 Hanko, Finland,

<sup>2</sup>Department of Environmental Sciences, University of Helsinki, PO Box 65, FI-00014 Helsinki, Finland, <sup>3</sup>Finnish Environment Institute, Marine Research Centre, PO Box 140, FI-00251 Helsinki, Finland and <sup>4</sup>Department of Biological and Environmental Science, PO Box 35, University of Jyväskylä, FI-40014 Jyväskylä, Finland

\*Corresponding author: Department of Environmental Sciences, University of Helsinki, Miss Enberg, Sara Viikinkaari 1, PO Box 65, FI-00014 Helsinki, Finland. Tel: +358 50 4486467; E-mail: [sara.enberg@helsinki.fi](mailto:sara.enberg@helsinki.fi)

**One sentence summary:** UVR in sea ice regulates algal biomass, vertical distribution, species composition and their photosynthetic activity; therefore, subsurface layers beneath the reach of UVR provide suitable growth conditions for sea ice algae.

**Editor:** Riks Laanbroek

## ABSTRACT

The effects of increased photosynthetically active radiation (PAR) and ultraviolet radiation (UVR) on species diversity, biomass and photosynthetic activity were studied in fast ice algal communities. The experimental set-up consisted of nine 1.44 m<sup>2</sup> squares with three treatments: untreated with natural snow cover (UNT), snow-free (PAR + UVR) and snow-free ice covered with a UV screen (PAR). The total algal biomass, dominated by diatoms and dinoflagellates, increased in all treatments during the experiment. However, the smaller biomass growth in the top 10-cm layer of the PAR + UVR treatment compared with the PAR treatment indicated the negative effect of UVR. *Scrippsiella* complex (mainly *Scrippsiella hangoei*, *Biecheleria baltica* and *Gymnodinium corollarium*) showed UV sensitivity in the top 5-cm layer, whereas *Heterocapsa arctica* ssp. *frigida* and green algae showed sensitivity to both PAR and UVR. The photosynthetic activity was highest in the top 5-cm layer of the PAR treatment, where the biomass of the pennate diatom *Nitzschia frigida* increased, indicating the UV sensitivity of this species. This study shows that UVR is one of the controlling factors of algal communities in Baltic Sea ice, and that increased availability of PAR together with UVR exclusion can cause changes in algal biomass, photosynthetic activity and community composition.

**Keywords:** UVR; sea ice; algae; photosynthetic activity; Baltic Sea

## INTRODUCTION

The sea ice is an extreme environment for the algae living within. Their primary production is controlled largely by availability of light, but algal responses are also depended on the optical properties of sea ice. The level of exposure to solar radiation

is dependent on the thickness of snow and ice cover, the structure of sea ice and the ice temperature, all of which influence the scattering properties (Buckley and Trodahl 1987; Perovich, Roesler and Pegau 1998; Perovich et al. 2002). In the Baltic sea ice, most of the irradiance is attenuated in the surface layers of

Received: 22 December 2014; Accepted: 20 August 2015

© FEMS 2015. All rights reserved. For permissions, please e-mail: [journals.permissions@oup.com](mailto:journals.permissions@oup.com)

the ice (approximately 10 cm) (Uusikivi et al. 2010). The granular structure of the surface ice is highly scattering and usually associated with high concentrations of absorbing materials, resulting in higher attenuation coefficients than in the columnar ice common to the deeper layers (Perovich, Roesler and Pegau 1998). Snow reflects a part of the incoming radiation, and the amount of reflected radiation is dependent on the snow properties, with the highest albedos in fresh dry snow (Perovich, Roesler and Pegau 1998; Perovich et al. 2002).

If future scenarios with warming climate and milder winters in the northern latitudes are realized (Helsinki Commission HELCOM 2013), resulting in a thinner ice sheet and snow cover, more solar radiation will penetrate into the ice. This will increase the availability not only of photosynthetically active radiation (PAR 400–700 nm) for photoautotrophic sea ice algae, but also the exposure to ultraviolet radiation (UVR 280–400 nm), which induces damages in DNA, reduces microalgal enzyme and protein production, decreases the velocity of cell movement and changes cellular stoichiometry by decreasing uptake and inhibiting utilization of inorganic nutrients (Häder and Häder 1991; Döhler 1992; Arts and Rai 1997). UVR also reduces photosynthetic activity in phytoplankton communities by decreasing the carbon assimilation rate (Kim and Watanabe 1993; Helbling, Villafañe and Holm-Hansen 1994). However, high concentrations of UV-absorbing mycosporine-like amino acids (MAAs) and high activity of antioxidant enzymes may protect phytoplankton under high levels of solar irradiance (Helbling et al. 1996; Rijstebil 2002; Ryan et al. 2002; Wang et al. 2009; Uusikivi et al. 2010; Piiparinen et al. 2015).

The movement of algae within sea ice is restricted, and the sea ice algae are probably unable to avoid changes in light environment in contrast to open water phytoplankton. Organisms in the upper layers of the ice are exposed to higher light intensities and to greater UVR doses than are organisms in the deeper layers. The high solar irradiance at the surface ice has been infrequently examined, since many light manipulation and UVR studies of sea ice algae have been conducted with polar sea ice and, hence, were focused on the bottom layers (McMinn, Ashworth and Ryan 1999; McMinn, Ryan and Gademann 2003; Juhl and Krembs 2010; Petrou et al. 2011; Ryan et al. 2012; Alou-Font et al. 2013; Lund-Hansen et al. 2014). The responses of the bottom ice algae to increase in solar irradiance (e.g. the change in biomass accumulation) are dependent on the thickness of the snow cover and photoacclimation state of the algae (McMinn, Ashworth and Ryan 1999; Juhl and Krembs 2010; Ryan et al. 2012). In the upper layers of sea ice, the light environment is different from that of the bottom layers and snow removal results in decline in algal biomass, indicating the importance of the snow cover in protecting the ice algae from high light intensities and UVA (Uusikivi et al. 2010; Piiparinen and Kuosa 2011).

The algal communities thriving in the brine channels of the Baltic sea ice contribute about 10% of primary production during the ice-covered season (Haecky and Andersson 1999). The ice algal biomass is usually dominated by diatoms and dinoflagellates (e.g. Hicckel 1969; Huttunen and Niemi 1986; Norman and Andersson 1994; Ikävalko and Thomsen 1997; Haecky, Jonsson and Andersson 1998; Haecky and Andersson 1999; Meiners et al. 2002; Rintala, Piiparinen and Uusikivi 2010), whereas small flagellates (<10 µm), despite high cell numbers, rarely dominate the algal biomass except in newly formed ice (Rintala, Piiparinen and Uusikivi 2010). Centric diatoms generally predominate in the upper layer communities (Kaartokallio et al. 2007; Piiparinen, Kuosa and Rintala 2010; Rintala, Piiparinen and Uusikivi 2010), which could be linked not only with snow ice providing larger habit-

able spaces for long-chain-forming centric diatoms (Piiparinen, Kuosa and Rintala 2010; Rintala, Piiparinen and Uusikivi 2010), but also with their more efficient protection mechanisms of photosystems under higher irradiances than are used by pennate diatoms (Ban et al. 2006). Karentz, Cleaver and Mitchell (1991) showed that centric diatoms are more resistant to UVR, due to their multiple small peripheral chloroplasts acting as additional screens for the light entering the cell, in contrast to the pennate diatoms, which have only two chloroplasts.

The variation in the UV sensitivity of various diatoms and flagellates, such as dinoflagellates, cryptophytes and euglenids, induces changes in the sea ice community composition (Gerber and Häder 1995; Villafañe et al. 1995; Davidson, Marchant and de la Mare 1996; Williamson et al. 2010). In Baltic Sea ice, UVA radiation (315–400 nm) decreases the chlorophyte and diatom biomasses in the surface layers of the ice, but does not affect their photosynthetic activity (Piiparinen and Kuosa 2011). The aim of this study was to investigate the effects of the full solar spectrum (PAR + UVR) on the ice algal community composition and photosynthetic activity and to estimate the role of UVR in these responses by including a treatment in which UVR was excluded. An *in situ* approach was selected to minimize the disturbances in the community studied and to obtain a natural light spectrum and levels.

## MATERIALS AND METHODS

### Study site, experimental set-up and sampling

The study was carried out as a 2-week *in situ* experiment on fast ice on the south-west coast of Finland (59° 50' 36 N, 23° 15' 07 E), in the Baltic Sea (Fig. 1a). Despite the brackish nature of the study area, mean salinity of 6, the ice resembles the oceanic sea ice with channels and pockets filled with saline brine. The experimental field was established on 28 February 2011 in the middle of a semi-enclosed, shallow bay (average depth 3 m) with 33- to 38-cm-thick fast ice covered uniformly by 4–6 cm of snow. The experimental set-up consisted of nine 1.44 m<sup>2</sup> squares, about 1 m apart and divided into three treatments (three replicates each) arranged in a 3 × 3 Latin square design (Fig. 1b) to account for potential horizontal patchiness. Three of the squares had natural snow cover throughout the experiment (untreated, UNT). Snow was removed from the remaining six squares, which three of them were exposed to the full solar spectrum (PAR + UVR treatment), and the three remaining squares (PAR treatment) were covered with UV filter film (No. 311413; Roscolab Ltd, London, England), which blocked the radiation below 390 nm but allowed about 82% transmission of wavelengths >390 nm (Piiparinen and Kuosa 2011). During the experiment, the ice thickness increased 0–5 cm and the snow cover on the UNT ice increased to 7–9 cm. Since the wind constantly carried some loose snow over the experimental field, the PAR and PAR + UVR treatments were cleared of snow and frost every day throughout the experiment. According to Hamre et al. (2004), the transmittance of the snow cover decreases fast in the first few centimetres of the snow. The treatments were expected to cause drastic but natural changes in the levels of solar UVR and PAR in the sea ice. The surface of the UNT ice was expected to receive <20% of the UVR and PAR incident to the experimental field, accounting for the attenuation by snow cover of >5 cm thickness during the experiment based on model calculations (Müller et al. submitted). The sea ice algae in the snow-free treatments (PAR + UVR and PAR) received the incident PAR directly without attenuation by snow. The algae in the PAR treatment received essentially no UVR, but those in the

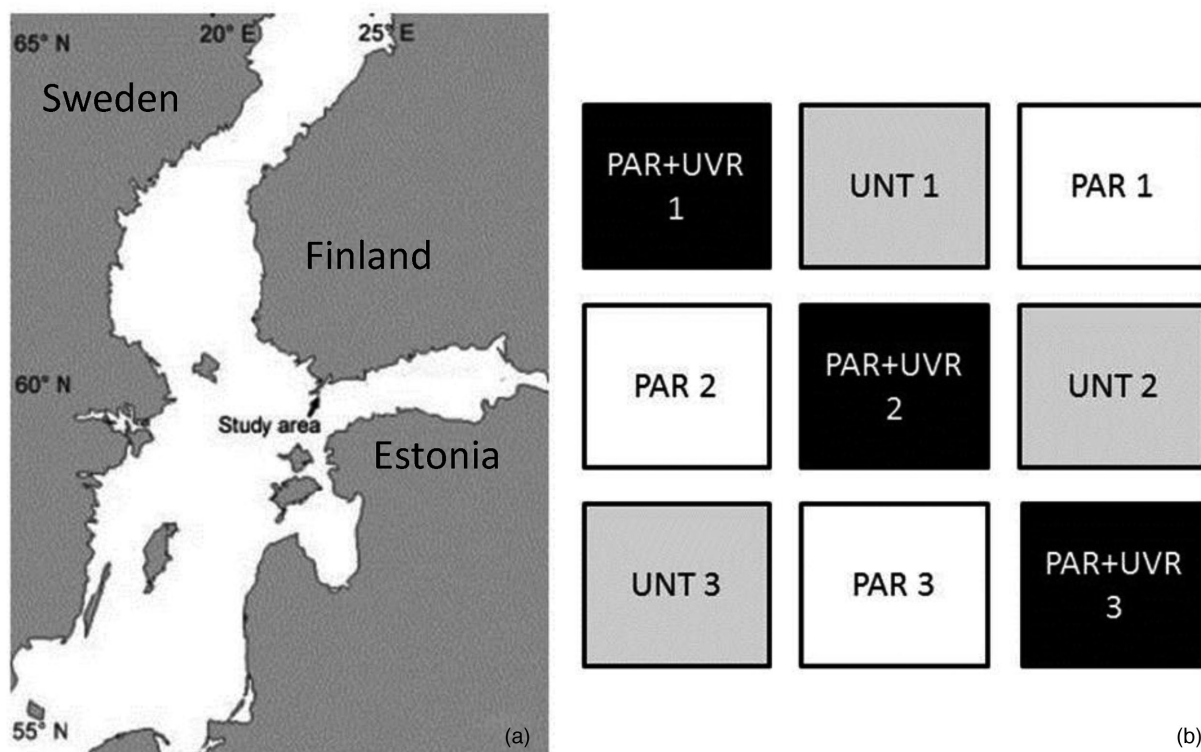


Figure 1. The study area on the left (a) and Latin square experimental design on the right (b).

PAR + UVR treatment were exposed to doses of UVR more than four times higher than that of the UNT ice.

The incoming radiation during the experiment was measured from 280 to 800 nm in 1-nm steps at 1-h intervals with a Macam SR991 spectroradiometer [Macam Photometrics Ltd (now Irradian Ltd), Tranent, West Lothian, UK] and air temperature at 0.5-h intervals with a GroWeather station (Davis Instruments Corp., Hayward, CA, USA) placed on the roof of Tvärminne Zoological Station about 200 m from the experiment field. The temperatures on the ice surface in all treatments were measured with three aluminium foil-covered temperature loggers (Hobo Pro v2; Onset Computer Corp., Bourne, MA, USA) (one logger per treatment) at 1-h intervals throughout the experiment. The loggers were placed between the ice surface and the snow (UNT), on top of the ice (PAR + UVR) and between the ice surface and the film (PAR).

The ice samples from all treatments were collected every 7 days (28 February, 7 March and 14 March). To ensure enough ice for all analyses and to reduce the effect of patchiness, five ice cores from each square were obtained, using a motorized Cold Regions Research and Engineering Laboratory (CRREL)-type ice-coring auger (9-cm internal diameter; Kovacs Enterprises, Roseburg, OR, USA). The core holes were sealed with frozen fresh ice cylinders to prevent damage to the sampling field, e.g. from lateral brine drainage via the drill holes. The thickness of each ice core was measured to 1-cm precision, and the ice cores were cut into four vertical pieces. The impact of UVR was assumed to be greatest in the surface layers of the ice, and thus the topmost 10-cm layer was sliced into two 5-cm pieces. The bottommost 10-cm pieces represented the bottom ice communities and the remaining intermediate parts of the cores were from 13 to 20 cm thick. After slicing the ice cores, the five ice pieces per layer

in each square were pooled in one sample and placed in plastic containers or in plastic tubing (Mercamer Oy, Vantaa, Finland) and transported in the dark to the laboratory, where they were crushed into smaller pieces and melted overnight without allowing the temperature of the sample to rise above +4°C. As suggested for Baltic sea ice samples in Rintala et al. (2014), the rapid melting without an addition of salinity buffers was selected to minimize algal growth, death and other biological processes. The bulk salinities were measured with a YSI 63 meter (Yellow Springs Instrument Inc., Yellow Springs, OH, USA).

For measuring the inorganic ( $\text{NH}_4$ ,  $\text{NO}_2 + \text{NO}_3$ ,  $\text{PO}_4$  and  $\text{SiO}_4$ ) and total nutrient (tot-N and tot-P) concentrations, the three replicate samples from each ice layer were pooled and determinations performed, using a Hitachi U-110 Spectrophotometer (Hitachi High-Technologies Corp., Tokyo, Japan) with standard protocols for seawater analysis (Koroleff 1976). The concentrations of dissolved nutrients were normalized to the mean bulk salinities to correct for salinity-related variations in the nutrient concentrations.

### Chlorophyll *a* and algal community

From each replicate ice sample, two 100 mL subsamples were filtered onto GF/F (Whatman, Sigma-Aldrich Co. LLC, St. Louis, MO, USA) filters, soaked to 96% v/v ethanol and kept in darkness overnight to extract chlorophyll *a* (chl *a*). The concentration of chl *a* was calculated from the chl *a* fluorescence measured with a Cary Eclipse spectrofluorometer [Varian Inc. (Agilent Technologies), Santa Clara, CA, USA] calibrated with pure chl *a* (HELCOM 1988).

Subsamples (100 mL) from each square were preserved with acid Lugol's solution for microscopic enumeration of algae.

Depending on the density of the sample, a volume of 50 or 10 mL was settled for 24 h, according to Ütermöhl (1958), and examined with a Leitz DM IL, Leica DM IL or Leica DMIRB inverted light microscope equipped with 10× oculars and 10× or 40× objectives (Leica Microsystems, Wetzlar, Germany). Large cells or colonies were counted with 100× magnification over an area that covered one third of the cuvette, and the abundance of small taxa was counted from 50 random fields with 400× magnification. Most of the small flagellates could not be identified to species level, and thus cells belonging to the classes Cryptophyceae, Euglenophyceae, Prasinophyceae and Prymnesiophyceae were counted at group level. The algal cell numbers were converted into carbon biomasses ( $\mu\text{g C L}^{-1}$ ) using species-specific biovolumes and carbon contents according to Olenina et al. (2006) and Menden-Deuer and Lessard (2000). The values gained were also used for calculating the biomass/chl *a* ratio ( $\mu\text{g C } [\mu\text{g chl a}]^{-1}$ ).

### Photosynthesis-irradiance response measurements

Photosynthetic activity was examined as a photosynthesis-irradiance response. The samples for each ice layer were pooled from three replicate squares. A method of Steemann Nielsen (1952) with modifications by Niemi et al. (1983) was used for calculating the carbon assimilation. Sample volumes of 3 mL with 50  $\mu\text{L}$   $\text{NaH}^{14}\text{CO}_3$  addition (final concentration 0.33  $\mu\text{Ci mL}^{-1}$ ) were incubated for 2 h under 16 different light intensities between 6 and 4087  $\mu\text{mol m}^{-2} \text{s}^{-1}$  with two dark controls in incubators cooled with cold water circulation. The incubation was stopped by adding 100  $\mu\text{L}$  of 37% formaldehyde to the samples. The unincorporated  $\text{NaH}^{14}\text{CO}_3$  was removed from the samples during the following 48 h by addition of 100  $\mu\text{L}$  of 1 N HCl. Insta-Gel Plus (PerkinElmer, Waltham, MA, USA) scintillation cocktail was added, and the incorporated radioactivity was measured with a Wallac WinSpectral 1414 scintillation counter (Wallac PerkinElmer, Turku, Finland). The total inorganic carbon was measured, using a Uras 3E carbon analyser (Electro-Dynamo AB, Helsingborg, Sweden), as explained by Salonen (1981). The carbon uptake rates were normalized to chl *a* ( $\mu\text{g C } [\mu\text{g chl a}]^{-1} \text{h}^{-1}$ ) and the photosynthetic efficiency ( $\alpha^b$ ), maximum photosynthetic capacity ( $P^b_m$ ), photoinhibition ( $\beta$ ) and the light saturation index ( $E_k$ ) were determined from photosynthesis-irradiance response curves, according to Platt, Gallegos and Harrison (1980). The superscript 'b' for  $\alpha^b$  and  $P^b_m$  denotes the normalization to chl *a*.

### Statistical analyses

A three-way analysis of variance (ANOVA), designed for Latin squares (treatment, row and column as fixed factors), was used to test the significance of the differences between treatments for chl *a*, total biomass and the biomass of most abundant algal taxa. Levene's test was used to test the homogeneity of variances, using the significance level  $P < 0.05$ . A parametric ANOVA and Tukey's *b* test in pairwise comparisons were used when the variances were homogenous, while a non-parametric Scheirer-Ray-Hare test with ranked data and the Mann-Whitney *U* test were used when the variances were unequal. The correlation between algal biomass and chl *a* concentrations was analysed with Pearson's correlation, using the significance level  $P < 0.05$ . All the procedures were performed in SPSS for Windows (version 22, IBM SPSS Statistics 2013; IBM Corp., Armonk, NY, USA).

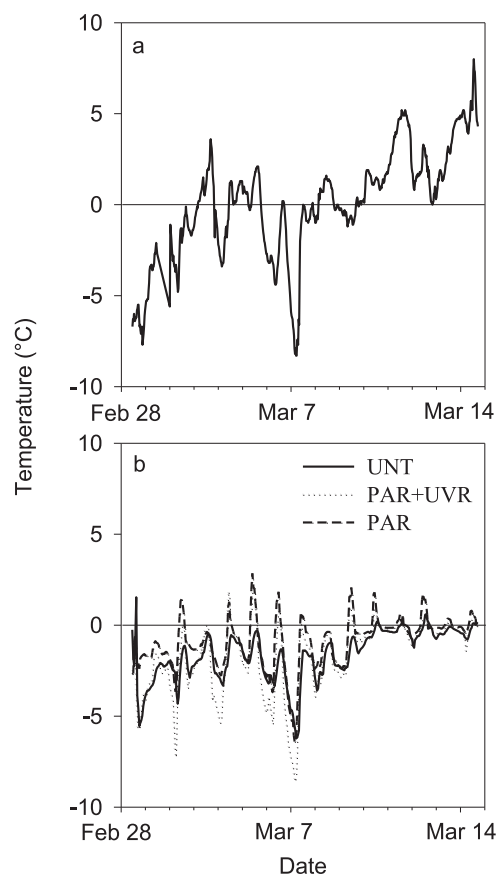


Figure 2. (a) Air and (b) ice surface temperatures ( $^{\circ}\text{C}$ ) in the various treatments during the experiment.

Table 1. Mean solar radiation (PAR + UVR) and UVB, UVA and PAR ( $\text{W m}^{-2}$ ) during the experiment.

	Feb 28–Mar 6	Mar 7–Mar 13
UVB (280–315 nm)	0.04	0.05
UVA (316–400 nm)	4.42	4.45
PAR (401–700 nm)	33.50	33.31
PAR + UVR (280–700 nm)	37.96	37.81

## RESULTS

### Physical environment and nutrients

The ice cover in the study area formed in early January 2011, about 8 weeks prior to the start of the experiment. During the experiment, the air temperature ranged from  $-8.2$  to  $+5.7^{\circ}\text{C}$  and increased towards the end of the experiment (Fig. 2a). The snow cover insulated the ice and hindered the fluctuation of temperature in the ice surface, seen as less variable surface temperatures of the UNT ice ( $-1.65 \pm 1.36^{\circ}\text{C}$  mean  $\pm$  sd) than in the PAR + UVR and PAR treatments ( $-1.66 \pm 2.00$  and  $-0.87 \pm 1.41^{\circ}\text{C}$ , respectively) (Fig. 2b). The mean incident solar irradiance on the study field was similar during both weeks (Table 1), but the increased cloudiness during the second week resulted in increased variation in the daily maximum PAR and UVR (52–250 and 8–30  $\text{W m}^{-2}$ , respectively) than in the first week (PAR 52–176 and UVR 8–22  $\text{W m}^{-2}$ , respectively; Fig. S1, Supporting Information).

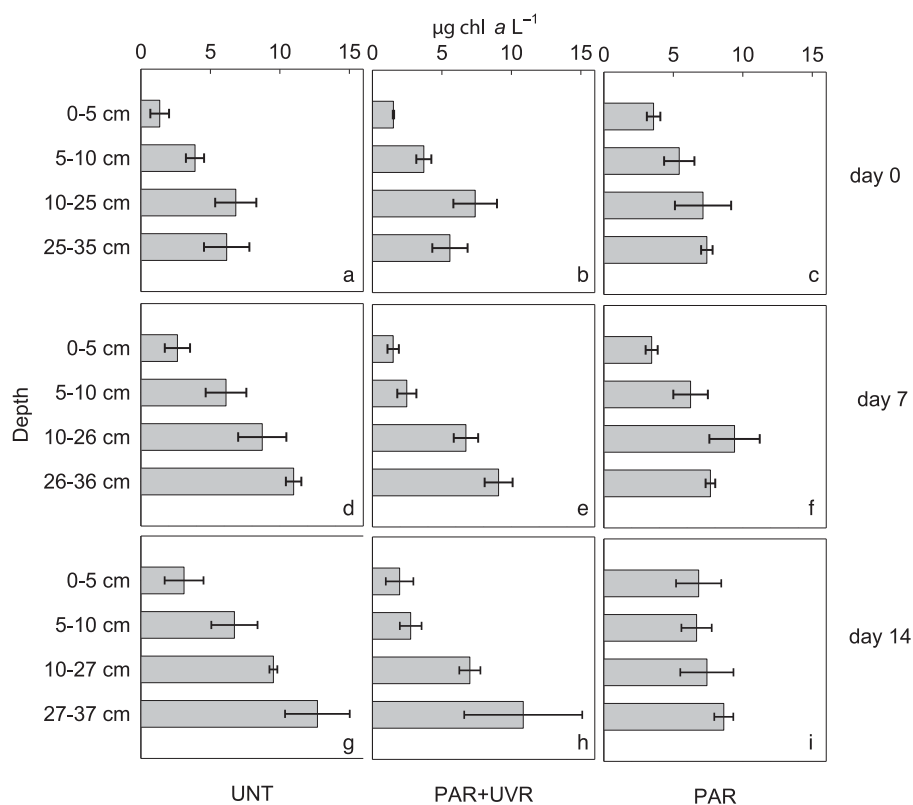


Figure 3. Mean chl *a* concentrations ( $\mu\text{g L}^{-1}$ )  $\pm$  standard deviations in the various treatments in each ice layer at each sampling.

Nutrient concentrations in the treatments over the duration of the experiment are given in Table S1 (Supporting Information). Except the high tot-N concentration in the surface of the PAR + UVR treatment, due to the atmospheric deposition, no obvious trends were evident in the data.

### Chlorophyll *a* and algal community

At the beginning of the experiment, the chl *a* concentration was lowest in the upper parts of the ice (Fig. 3a–c). The chl *a* concentration was uniform in the experimental field, except the 5- to 10-cm layer, where significant differences were found among the squares assigned for the treatments (Latin square ANOVA,  $P < 0.05$ ).

On day 7, the chl *a* concentration in the top 5 cm was significantly lower in the PAR + UVR treatment than in the PAR treatment (Latin square ANOVA  $P < 0.05$ , Tukey's *b*  $P < 0.05$ ) (Fig. 3e and f), but by the end of the experiment, the difference had diminished (Fig. 3h and i). At the end of the experiment, the vertical distribution of the chl *a* concentration differed between the treatments. In the UNT ice, the chl *a* concentration increased linearly towards the ice bottom (Fig. 3g), while in the PAR + UVR treatment the increase was more exponential in shape (Fig. 3h), and in the PAR treatment the chl *a* concentration was distributed evenly throughout the ice (Fig. 3i). The algal biomass correlated positively with the chl *a* concentration (Pearson's correlation,  $n = 108$ ,  $r^2 = 0.63$ ,  $P < 0.01$ ), resulting in a similar depth distribution of the biomass and chl *a* during the experiment. The lowest algal biomass was in the top 5 cm of the PAR + UVR treatment on days 7 and 14, but was similar to that of chl *a*; a significant difference between the PAR + UVR and PAR treatments was found only on day 7 (Latin square ANOVA  $P < 0.05$ , Tukey's *b*  $P < 0.05$ , Fig. 4).

At the beginning of the experiment, the highest biomass/chl *a* ratios were in the surface layers. At the end of the experiment, the highest biomass/chl *a* ratios in the PAR + UVR and PAR treatment were observed in the bottom 10-cm layer, but in the UNT ice the ratio was similar throughout the layers (Table 2).

The ice algal community consisted mainly of dinoflagellates, diatoms, green algae and unidentified flagellates (Fig. 4, Table S2, Supporting Information). Unidentified flagellates  $< 20 \mu\text{m}$  dominated the ice algal cell densities at 50–60% (data not shown), but their biomass comprised less than 10% of the total biomass. Instead, the algal biomass was dominated by diatoms (40–60%) and dinoflagellates (20–40%) (Fig. 4). The most abundant diatoms were pennate species, especially unicellular or chain-forming colonies of *Pauliella taeniata* (Grunow) Round & Basson/*Navicula Bory de Saint-Vincent* sp. and unicellular or arborescent colonies of *Nitzschia frigida* Grunow. On day 14, a high diatom biomass accumulation was observed in the top 5-cm layer in the PAR treatment, where the pennate diatom *N. frigida* occurred as large colonies (Fig. S2, Supporting Information) with significantly higher biomass than in the PAR + UVR treatment (Latin square ANOVA  $P < 0.01$ , Tukey's *b*  $P < 0.05$ ). *Pauliella taeniata*/*Navicula* sp., on the other hand, was equally abundant among the treatments and throughout the experiment (Fig. S2, Supporting Information).

In total, the dinoflagellate biomass among the treatments did not differ significantly in any layer during the experiment (Latin square ANOVA  $P > 0.05$ ) (Fig. 4a–i). However, some differences were found at the group/species level. On day 14, the biomass of the *Scrippsiella* complex, which consisted of pigmented dinoflagellates unidentifiable to species level (mainly *Scrippsiella hangoei* (J.Schiller) J.Larsen, *Biecheleria baltica* Moestrup, Lindberg & Daugbjerg and *Gymnodinium corollarium* A. M. Sundström, Kremp &

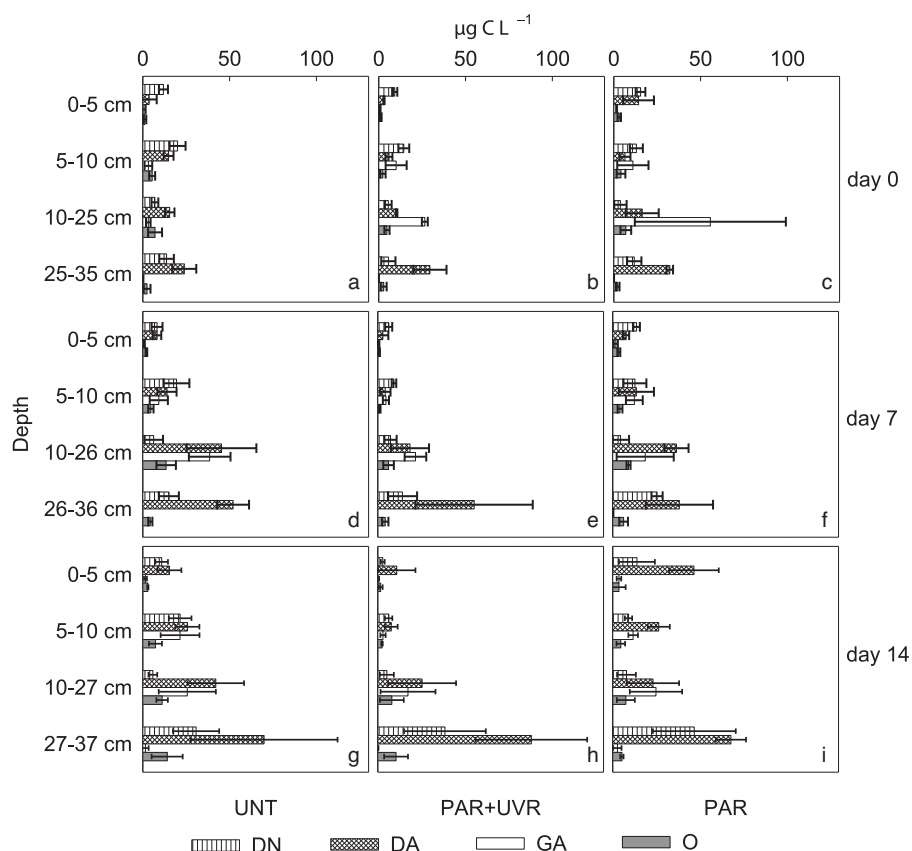


Figure 4. Mean biomasses ( $\mu\text{g C L}^{-1}$ )  $\pm$  standard deviations of Dinophyceae (DN), Diatomophyceae (DA), green algae (GA) and others (O) in the various treatments in each ice layer at each sampling.

Daugbjerg), was higher in the UNT ice and PAR treatment than in the PAR + UVR treatment in the top 5-cm layer (Scheirer-Ray-Hare  $P = 0.05$ , Mann Whitney U  $P = 0.05$ ) (Fig. S3, Supporting Information). The predominant dinoflagellates identified were *Heterocapsa arctica* Horiguchi ssp. *frigida* Rintala & G. Hällfors and species from the genus *Prorocentrum* Ehrenberg. On day 14, the biomass of *H. arctica* ssp. *frigida* was significantly higher in the UNT ice than in the PAR + UVR and PAR treatments in the 5- to 10-cm layer (Latin square ANOVA  $P < 0.05$ , Tukey's  $b P < 0.05$ ) (Fig. S4, Supporting Information).

Green algae (mostly *Chlamydomonas caudata* Wille and *Klebsormidium flaccidum* (Kützing) P.C. Silva et al.) were present in all ice layers, especially in the 5–10 cm and middle layer of the ice (Fig. 4a–i). On day 14, the total biomass of green algae in the 5- to 10-cm layer was significantly higher in the UNT ice and PAR treatment than in the PAR + UVR treatment (Scheirer-Ray-Hare  $P < 0.05$ , Mann Whitney U  $P < 0.05$  and  $P = 0.05$ , respectively; Fig. 4g–i). The biomass of separate green algae species in the ice did not differ between treatments (Latin square ANOVA  $P > 0.05$ ).

### Photosynthetic activity

During the experiment, the highest  $\alpha^b$  values were found in the layers below 10 cm in every treatment, whereas the depth of the  $P_m^b$  varied between the treatments (Fig. 5a–l; Table 2). The highest  $E_k$  value was always in the upper 10 cm (Fig. 5a–f; Table 2). On day 7, there were no clear differences in photosynthetic activity parameters between the treatments in the top 5-cm layer (Table 2), while in the 5- to 10-cm layer,  $\alpha^b$  and  $P_m^b$  were smaller

than on day 0. In the bottom layer, the  $P_m^b$  was higher than on day 0, but the highest  $P_m^b$  value was observed in the 10- to 26-cm layer in the PAR + UVR treatment. On day 14, the  $\alpha^b$  values were similar in the PAR and PAR + UVR treatments throughout the ice column, but the  $P_m^b$  and  $E_k$  values in the 0- to 5-cm layer of the PAR treatment were 1.6-fold higher than those in the PAR + UVR treatment (Table 2). The UNT ice differed from the exposed treatments, and on day 14 the  $\alpha^b$  value in the top 5 cm was half of that in the treated ice, and the  $P_m^b$  value was 1.4–2.2 times lower than in the treated ice (Fig. 5c, Table 2). The  $E_k$  value in the 0- to 5-cm layer was lower in the PAR + UVR treatment ( $135 \mu\text{mol m}^{-2} \text{s}^{-1}$ ) than in the UNT ice ( $195 \mu\text{mol m}^{-2} \text{s}^{-1}$ ) and the PAR treatment ( $212 \mu\text{mol m}^{-2} \text{s}^{-1}$ ). At high light intensities, photosynthesis in the bottom 10-cm layer was inhibited in every treatment during the experiment. In the top 5 cm, the communities both in the PAR and PAR + UVR treatments exhibited photoinhibition on day 14, but the  $\beta$  value was twice as high in the PAR + UVR treatment as in the PAR treatment (Table 2).

### DISCUSSION

Snow removal led to large changes in the amount of solar radiation in sea ice. The algae in the UNT ice received one fifth of the PAR under the snow cover compared to the snow-free treatment. The contrast between the PAR and PAR + UVR treatments was also drastic, since the PAR + UVR treatment received the incident UVR without attenuation by snow, while the algae of the PAR treatment received no UVR. The PAR + UVR treatment received also more PAR than the PAR treatment, where the foil

**Table 2.** Range of biomass/chl *a* ratios ( $\mu\text{g C } [\mu\text{g chl } a]^{-1}$ ), photosynthetic activity parameters and  $R^2$  values of the fitted models in the various treatments in each ice layer at each sampling. The photosynthetic efficiency ( $\alpha^b$ ) ( $\mu\text{g C } [\mu\text{g chl } a]^{-1} \text{ h}^{-1}$  [ $\mu\text{mol m}^{-2} \text{ s}^{-1}]^{-1}$ ), maximum photosynthetic capacity ( $P_m^b$ ) ( $\mu\text{g C } [\mu\text{g chl } a]^{-1} \text{ h}^{-1}$ ), photoinhibition ( $\beta$ ) ( $\mu\text{g C } [\mu\text{g chl } a]^{-1} \text{ h}^{-1}$  [ $\mu\text{mol m}^{-2} \text{ s}^{-1}]^{-1}$ ) and light saturation index ( $E_k$ ) ( $\mu\text{mol m}^{-2} \text{ s}^{-1}$ ). Single asterisk (\*) denotes significant photoinhibition ( $P < 0.05$ ) and two asterisks (\*\*) highly significant photoinhibition ( $P < 0.01$ ).

	Depth (cm)	C/chl <i>a</i> ratio	$\alpha^b$	$P_m^b$	$\beta$	$E_k$	$R^2$
<b>day 0</b>							
<b>UNT</b>							
	0–5	12.00–15.31	0.0032	0.64	0.00010	199	0.67
	5–10	9.04–13.19	0.0064	0.83	0.00005	129	0.90
	10–25	3.94–5.77	0.0066	0.67	0.00004	101	0.95
	25–35	5.80–8.31	0.0116	0.69	0.00050 *	60	0.92
<b>PAR + UVR</b>							
	0–5	7.96–10.48	0.0061	0.74	0.00010	121	0.74
	5–10	7.87–10.53	0.0036	0.58	0.00007	161	0.70
	10–25	4.61–8.00	0.0055	0.73	0.00010	132	0.89
	25–35	5.96–8.04	0.0076	0.53	0.00040 **	70	0.94
<b>PAR</b>							
	0–5	8.75–11.02	0.0044	0.61	0.00010	139	0.78
	5–10	4.49–8.21	0.0050	0.75	0.00010	149	0.82
	10–25	5.29–14.46	0.0066	0.75	0.00005	114	0.92
	25–35	5.64–7.52	0.0116	0.72	0.00010 *	62	0.89
<b>day 7</b>							
<b>UNT</b>							
	0–5	6.48–9.41	0.0025	0.49	0.00010 **	196	0.91
	5–10	6.63–8.77	0.0036	0.46	0.00020	129	0.71
	10–26	7.01–15.03	0.0081	0.70	0.00030 **	86	0.96
	26–36	5.16–7.35	0.0085	0.46	0.00060 **	54	0.97
<b>PAR + UVR</b>							
	0–5	5.98–9.10	0.0025	0.36	0.00030	145	0.81
	5–10	7.14–8.44	0.0013	0.23	0.00005 *	179	0.91
	10–26	6.77–8.60	0.0065	0.90	0.00009	138	0.97
	26–36	3.71–11.44	0.0085	0.87	0.00030 **	103	0.98
<b>PAR</b>							
	0–5	6.97–8.72	0.0044	0.54	0.00010 *	123	0.81
	5–10	5.03–9.27	0.0034	0.53	0.00010	157	0.83
	10–26	6.26–8.86	0.0082	0.80	0.00010	98	0.92
	26–36	6.32–11.50	0.0051	0.62	0.00020	121	0.90
<b>day 14</b>							
<b>UNT</b>							
	0–5	9.18–13.03	0.0027	0.53	0.00005	195	0.93
	5–10	9.55–11.94	0.0029	0.58	0.00008	199	0.89
	10–27	6.08–11.13	0.0097	1.02	0.00020 **	106	0.98
	27–37	6.34–12.16	0.0058	0.44	0.00040 **	77	0.93
<b>PAR + UVR</b>							
	0–5	3.38–9.59	0.0052	0.70	0.00020	135	0.78
	5–10	6.02–7.64	0.0026	0.59	0.00010 *	225	0.94
	10–27	4.09–13.62	0.0069	0.81	0.00000	117	0.91
	27–37	8.23–19.28	0.0064	0.77	0.00010 *	120	0.97
<b>PAR</b>							
	0–5	8.43–11.40	0.0054	1.15	0.00010 *	212	0.96
	5–10	6.95–8.48	0.0022	0.60	0.00006	270	0.94
	10–27	5.87–10.83	0.0054	0.67	0.00005	124	0.98
	27–37	11.95–17.83	0.0070	0.60	0.00030 **	86	0.96

reduced PAR by 18%. The elevated PAR by 18% did not likely cause any photoinhibition to the algae examined, since such photoinhibition by PAR was absent in the photosynthesis-irradiance response measurements at the levels ( $<1000 \mu\text{mol m}^{-2} \text{ s}^{-1}$ ) found in surface ice (Fig. 5a–f; Uusikivi et al. 2010). Photosynthesis instead is sensitive to UVR (e.g. Cullen, Neale and Lesser 1992), which attenuates more steeply than PAR and is present in high levels only at depths  $<10$  cm in Baltic Sea ice (Uusikivi et al. 2010). In this study, algae responded to light treatments only in the

surface layers (0–5 and 5–10 cm), where UVR can be found, but not in the bottom layer with negligible UVR.

### Effect of PAR and UVR on chl *a* concentration and total algal biomass

The Baltic Sea ice algal biomass accumulation follows the seasonal increase in solar radiation, with peak biomass in March (Kaartokallio 2004). The chl *a* concentration and algal biomass

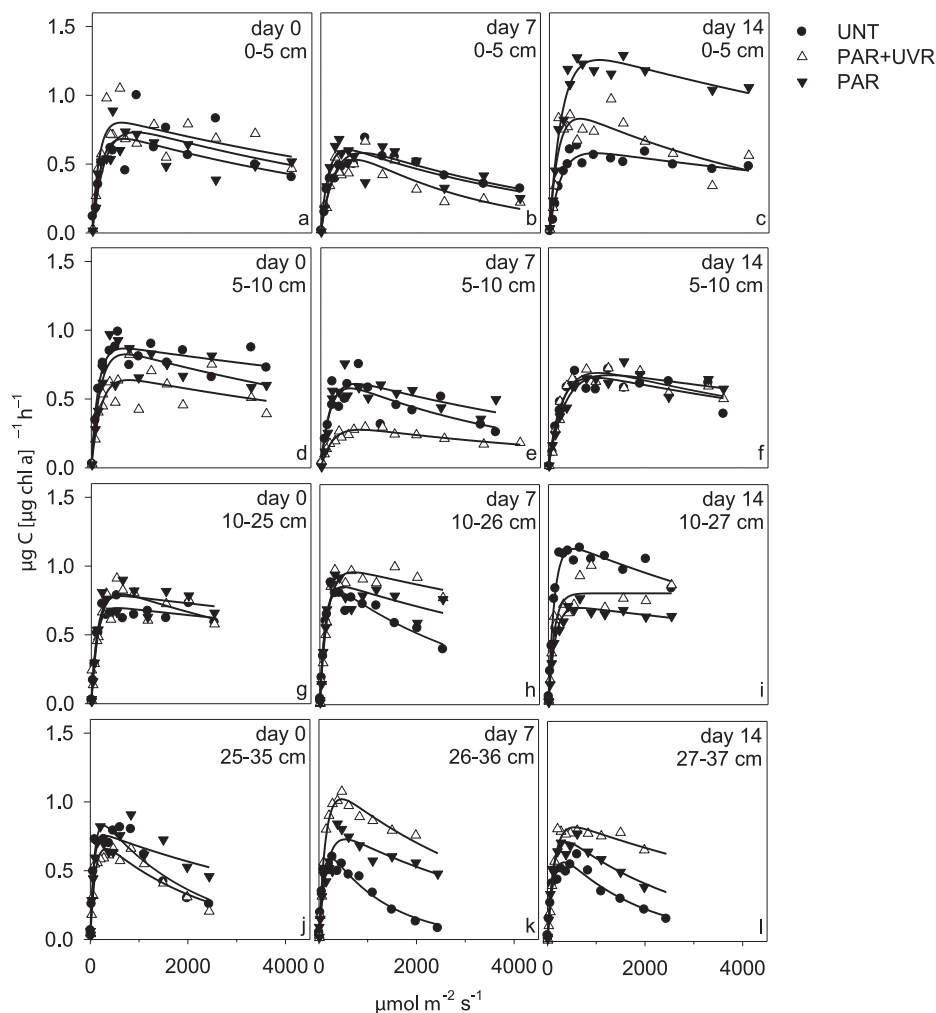


Figure 5. Photosynthesis-irradiance response curves in the various treatments in each ice layer at each sampling.

at the beginning of our experiment were similar to other measurements in early spring fast ice in the Baltic Sea (Norrman and Andersson 1994; Haecky, Jonsson and Andersson 1998; Haecky and Andersson 1999; Piiparinen and Kuosa 2011). The higher chl *a* concentration in the top 5 cm in the PAR treatment than in that of the UNT ice indicates that production increases under high light intensity when UVR is excluded. In earlier study at the same site, the concentration of chl *a* in the surface ice was higher under the snow cover than without the snow under the same UVR filter used in this study (Piiparinen and Kuosa 2011). The snow cover of the UNT ice in the present study likely protected the surface community from UVR, since the chl *a* concentration and algal biomass were higher in the top 5-cm layer in the snow-covered ice than in the PAR + UVR treatment, which was exposed to full solar radiation.

The biomass/chl *a* ratio of unicellular algae is dependent on the species and their physiological state as a consequence of photoacclimation to changing irradiances (Hegseth 1989). The biomass/chl *a* ratio in Baltic sea ice algae increases steadily from early March until ice breakup in late April (Haecky, Jonsson and Andersson 1998). At the beginning of this experiment, the low biomass/chl *a* ratio in the bottom 10-cm layer indicated photoacclimation of bottom ice communities to low light

conditions, while the removal of snow resulted in a higher ratio in the manipulated treatments. This indicates that the bottom ice assemblages became acclimated to higher light levels during the experiment. At the ice surface, removal of the snow cover did not increase the biomass/chl *a* ratio, indicating that the surface communities were already acclimated to higher light intensities and that the change in radiation (PAR and UVR) did not affect the ratio.

#### Effect of PAR and UVR on community composition

Although the algal biomass was similar to that of previous findings for early spring ice, the community composition was dominated by diatoms and dinoflagellates more typical of the late season community (Norrman and Andersson 1994; Haecky and Andersson 1999; Rintala et al. 2006; Kaartokallio et al. 2007; Piiparinen and Kuosa 2011). Centric diatoms generally predominate in the upper layer community (Kaartokallio et al. 2007; Piiparinen, Kuosa and Rintala 2010; Rintala, Piiparinen and Uusikivi 2010) and one of the plausible reasons is their ability to tolerate UVR better than pennate diatoms (Karentz, Cleaver and Mitchell 1991; Ban et al. 2006). However, in this study the ice



communities were dominated by pennate diatoms and the biomass of centric diatoms was low. When the sea ice was exposed to increased levels of incoming radiation (PAR + UVR), the sympagic community composition resembled that of the UNT ice, where diatoms and dinoflagellates were the most predominant taxa. This was similar to that of the previous studies mentioned above, with the exception that the pennate diatoms were encountered more frequently than the centric diatoms, and the exclusion of UVR increased the amount of pennate diatoms. Thus, we could not confirm whether centric diatoms tolerate more UVR than pennate diatoms.

The pennate diatom *N. frigida* showed clear UV sensitivity by increasing in biomass in the top 5 cm of the PAR treatment, while decreasing in the PAR + UVR treatment. This is in line with previous studies, in which the exposure to UVR decreased the amount of light-harvesting pigments of *N. closterium* (Ehrenberg) W. Smith (now accepted as *Ceratoneis closterium* Ehrenberg) (Buma et al. 1996), gliding motility of *N. linearis* (C. Agardh) W. Smith (Moroz et al. 1999) and photosynthetic rate of *N. palea* (Kützing) W. Smith and other *Nitzschia* Hassall species (Arts and Rai 1997; Nilawati, Greenberg and Smith 1997; Wulff et al. 2000), as well as lead to a loss of *N. longissima* (Brébisson) Ralfs (Santas et al. 1998). This study with *N. frigida* further emphasizes the sensitivity of *Nitzschia* sp. to UVR. However, this UV sensitivity may not be applicable to all pennate diatoms, since the chain-forming pennate diatom *P. taeniata/Navicula* sp. was abundant throughout the ice column and also in the top 5-cm layer, but was not sensitive to UVR during the experiment.

In our study, the dinoflagellates as a group showed no responses to higher PAR or UVR, but some responses were seen in the *Scrippsiella* complex and *H. arctica* ssp. *frigida*. The biomass of the *Scrippsiella* complex increased in the top 5 cm of the UNT ice and PAR treatment, indicating that the *Scrippsiella* complex did not benefit from increased PAR, but that they were UV sensitive. In this experiment, the biomass of *H. arctica* ssp. *frigida* was higher in the 5- to 10-cm layer of UNT ice than in the treatments with elevated PAR. Dinoflagellates may benefit from higher light intensities (Kim et al. 2008), but they can also be extremely light sensitive (López-Rosales et al. 2014) or adapt to a wide range of irradiances (Baek, Shimode and Kikuchi 2008). In addition, UVR inhibits the growth rate of marine dinoflagellate species, but the response varies between species (Ekelund 1991). For example, exposure of *H. triquetra* (Ehrenberg) F. Stein to UVR increased MAA synthesis and inhibited carbon fixation, indicating possible UV sensitivity (Wangberg, Persson and Karlson 1997; Helbling et al. 2008). The UV sensitivity of *H. arctica* ssp. *frigida* in our study may have been masked by the effect of PAR in the PAR + UVR treatment, since the species did not benefit from higher light intensities in the PAR treatment.

In our study, the biomass of green algae in the 0- to 5-cm layer was small and similar in all treatments. This is unlike previous studies, in which green algae grew better under higher irradiance, but were sensitive to UVR (Richardson, Beardall and Raven 1983; Piiparinen and Kuosa 2011). However, green algae may not have benefitted from high PAR in the top 5-cm layer, because the biomass of green algae in the PAR treatment was no higher than in the PAR + UVR treatment. Green algae in the 5- to 10-cm layer grew better in the UNT and PAR treatments than in the PAR + UVR treatment, indicating negative response to UVR. The same effect of UVR was not observed below the 10-cm layer, which indicates that the effect of UVR does not penetrate to the deeper layers.

## Effect of PAR and UVR on photosynthetic activity

After 7 days' exposure to the increased PAR + UVR levels, there were clear decreases in both  $\alpha^b$  and  $P^b_m$ , indicating that the increased UVR caused changes in the community in the top 10 cm of the ice. The community at the depth of 5–10 cm was able to recover after 14 days. This recovery was likely related to the production of MAAs and deposition of atmospheric particles, which increased the attenuation of UVR (Piiparinen et al. 2015).

The 2-fold higher  $P^b_m$  level on day 14 in the top 5 cm of the PAR treatment than in that of the UNT ice and PAR + UVR reflected the dominance of *N. frigida* in the PAR treatment. The UVR-induced differences in the community composition of the PAR and PAR + UVR treatments did not affect the  $\alpha^b$  level. In the 5- to 10-cm layer, the community composition at the group level was more similar between treatments and resulted in nearly identical photosynthesis-irradiance curves. The lower  $P^b_m$  level in the bottom layer of the UNT ice was likely due to the lowered availability of PAR than that of the PAR + UVR and PAR treatments resulting from the snow layer on the ice. These findings are in concordance with the previous studies from the Baltic Sea, in which bottom ice communities have been associated with smaller  $P^b_m$  values than those of the surface communities (Piiparinen, Kuosa and Rintala 2010; Rintala, Piiparinen and Uusikivi 2010; Piiparinen and Kuosa 2011). The low biomass and decreased self-shading in the upper layers of the PAR + UVR treatment likely resulted in better light penetration and increased amounts of PAR in the deeper layers. This is seen as higher  $\alpha^b$  and  $P^b_m$  levels of the PAR + UVR treatment below 10 cm than those of the PAR treatment. In polar sea areas, the photosynthetic activity is often measured only from the bottom ice assemblages, because most of the biomass is in the bottom layer of the ice (e.g. McMin, Ryan and Gademann 2003). In Baltic Sea ice, where the ice is thinner than in polar areas and the biomass is divided more evenly throughout the ice, measuring photosynthetic activity only in the bottom ice layer could result in underestimation of the responses of increased UVR to the entire ice community.

The photoinhibition of the bottom ice communities is in concordance with previous findings (Piiparinen, Kuosa and Rintala 2010; Rintala, Piiparinen and Uusikivi 2010; Piiparinen and Kuosa 2011). In our experiment, the highest light intensities in the incubators were twice the natural light levels, which at the surface of the Baltic Sea can be as much as  $2000 \mu\text{mol m}^{-2} \text{s}^{-1}$  in summer (Müller 2004). Despite the differences in the photosynthetic activity between the ice layers, the maximum level of photosynthesis was reached at incident light levels, meaning that the surface and bottom communities photosynthesized with equal maximum efficiency.

Similar to the values obtained by Piiparinen, Kuosa and Rintala (2010), Rintala, Piiparinen and Uusikivi (2010) and Piiparinen and Kuosa (2011), the largest  $E_k$  value was in the top 5 cm and the smallest in the bottom of the ice at the beginning of the experiment, indicating that the surface communities were acclimated to higher light intensities, whereas the bottom communities were shade-acclimated. At the end of the experiment, the largest  $E_k$  values were in the 5- to 10-cm layer in the treated ice, which indicates that the PAR intensities were too high in the top 5-cm layer without the snow cover, but the photosynthesis-irradiance incubations revealed that the ice algae were able to photosynthesize even at irradiance levels as high as  $1000\text{--}1500 \mu\text{mol m}^{-2} \text{s}^{-1}$ , whilst anything less than about  $500 \mu\text{mol m}^{-2} \text{s}^{-1}$  was not high enough to satisfy their photosynthetic demands.

## SUPPLEMENTARY DATA

Supplementary data are available at FEMSEC online.

## ACKNOWLEDGEMENTS

We would like to thank MSc. Elina Kari, Doc. Janne Soininen and Dr Joanna Norkko for their help during the field work and in the preparation of the manuscript. We also thank Dr James Thompson for the detailed language check. In addition, JMR, RA and SE thank the Institutum Romanum Finlandiae, Villa Lante, in Rome for their hospitality during our visit at the initiation writing phase of this manuscript.

## FUNDING

The Walter and Andrée de Nottbeck Foundation provided financial support for this work. The field and laboratory work was made possible by the facilities at Tvärminne Zoological Station, University of Helsinki.

**Conflict of interest.** None declared.

## REFERENCES

- Alou-Font E, Mundy C-J, Roy S, et al. Snow cover affects ice algal pigment composition in the coastal Arctic Ocean during spring. *Mar Ecol-Prog Ser* 2013;**474**:89–104.
- Arts M, Rai H. Effects of enhanced ultraviolet-B radiation on the production of lipid, polysaccharide and protein in three freshwater algal species. *Freshwater Biol* 1997;**38**:597–610.
- Baek SH, Shimode S, Kikuchi T. Growth of dinoflagellates, *Ceratium furca* and *Ceratium fusus* in Sagami Bay, Japan: the role of temperature, light intensity and photoperiod. *Harmful Algae* 2008;**7**:163–73.
- Ban A, Aikawa S, Hattori H, et al. Comparative analysis of photosynthetic properties in ice algae and phytoplankton inhabiting Franklin Bay, the Canadian Arctic, with those in mesophilic diatoms during CASES 03-04. *Polar Biosci* 2006;**19**:11–28.
- Buckley RG, Trodahl HJ. Thermally driven changes in the optical properties of sea ice. *Cold Reg Sci Technol* 1987;**14**:201–4.
- Buma AGJ, Zemmeling HJ, Sjollem K, et al. UVB radiation modifies protein and photosynthetic pigment content, volume and ultrastructure of marine diatoms. *Mar Ecol-Prog Ser* 1996;**142**:47–54.
- Cullen JJ, Neale PJ, Lesser MP. Biological weighting function for the inhibition of phytoplankton photosynthesis by ultraviolet radiation. *Science* 1992;**258**:646–50.
- Davidson AT, Marchant HJ, de la Mare WK. Natural UVB exposure changes the species composition of Antarctic phytoplankton in mixed culture. *Aquat Microb Ecol* 1996;**10**:299–305.
- Döhler G. Impact of UV-B radiation on uptake of N-ammonia and N-nitrate by phytoplankton of the Wadden Sea. *Mar Biol* 1992;**112**:485–9.
- Ekelund NGA. The effects of UV-B radiation on dinoflagellates. *J Plant Physiol* 1991;**138**:274–8.
- Gerber S, Häder DP. Effects of enhanced solar irradiation on chlorophyll fluorescence and photosynthetic oxygen production of five species of phytoplankton. *FEMS Microbiol Ecol* 1995;**16**:33–42.
- Häder DP, Häder M. Effects of solar and artificial u.v. radiation on motility and pigmentation in the marine *Cryptomonas maculata*. *Environ Exp Bot* 1991;**31**:33–41.
- Haecky P, Andersson A. Primary and bacterial production in sea ice in the northern Baltic Sea. *Aquat Microb Ecol* 1999;**20**:107–18.
- Haecky P, Jonsson S, Andersson A. Influence of sea ice on the composition of the spring phytoplankton bloom in the northern Baltic Sea. *Polar Biol* 1998;**20**:1–8.
- Hamre B, Winther J-G, Gerland S, et al. Modeled and measured optical transmittance of snow-covered first-year sea ice in Kongsfjorden, Svalbard. *J Geophys Res* 2004;**109**:C10006.
- Hegseth EN. Photoadaptation in marine arctic diatoms. *Polar Biol* 1989;**9**:479–86.
- Helbling EW, Buma AGJ, van de Poll W, et al. UVR-induced photosynthetic inhibition dominates over DNA damage in marine dinoflagellates exposed to fluctuating solar radiation regimes. *J Exp Mar Biol Ecol* 2008;**365**:96–102.
- Helbling EW, Chalker BE, Dunlap WC, et al. Photoacclimation of Antarctic marine diatoms to solar ultraviolet radiation. *J Exp Mar Biol Ecol* 1996;**204**:85–101.
- Helbling EW, Villafañe V, Holm-Hansen O. Effects of ultraviolet radiation on Antarctic marine phytoplankton photosynthesis with particular attention to the influence of mixing. *Antarct Res Ser* 1994;**62**:207–27.
- HELCOM. Guidelines for the Baltic monitoring programme for the third stage; Part D. Biological determinants. *Balt Sea Environ Proc* 1988;**27D**:16–23.
- HELCOM. Climate change in the Baltic Sea area: HELCOM thematic assessment in 2013. *Balt Sea Environ Proc* 2013;**137**:66.
- Hickel W. Planktologische und hydrographisch-chemische Untersuchungen in der Eckernförder Bucht (westliche Ostsee) während und nach der Vereisung in extrem kalten Winter 1962/1963. *Helgoland Wiss Meer* 1969;**19**:318–31.
- Huttunen M, Niemi Å. Sea-ice algae in the Northern Baltic Sea. *Memo Soc Flora Fauna Fenn* 1986;**62**:58–62.
- Ikävalko J, Thomsen HA. The Baltic Sea ice biota (March 1994): a study of the protistan community. *Eur J Protistol* 1997;**33**:229–43.
- Juhl AR, Krembs C. Effects of snow removal and algal photoacclimation on growth and export of ice algae. *Polar Biol* 2010;**33**:1057–65.
- Kaartokallio H. Food web components, and physical and chemical properties of Baltic Sea ice. *Mar Ecol-Prog Ser* 2004;**273**:49–63.
- Kaartokallio H, Kuosa H, Thomas DN, et al. Biomass, composition and activity of organism assemblages along a salinity gradient in sea ice subjected to river discharge in the Baltic Sea. *Polar Biol* 2007;**30**:183–97.
- Karentz D, Cleaver JE, Mitchell DL. Cell survival characteristics and molecular responses of Antarctic phytoplankton to ultraviolet-B radiation. *J Phycol* 1991;**27**:326–41.
- Kim DS, Watanabe Y. The effect of long wave ultraviolet radiation (UV-A) on the photosynthetic activity of natural population of freshwater phytoplankton. *Ecol Res* 1993;**8**:225–34.
- Kim S, Kang YG, Kim HS, et al. Growth and grazing responses of the mixotrophic dinoflagellate *Dinophysis acuminata* as functions of light intensity and prey concentration. *Aquat Microb Ecol* 2008;**51**:301–10.
- Koroleff F. Determination of nutrients. In: Grasshoff K (ed.). *Methods of Seawater Analysis*. Weinheim: Verlag Chemie, 1976, 117–81.
- López-Rosales L, Gallardo-Rodríguez JJ, Sánchez-Mirón A, et al. Simultaneous effect of temperature and irradiance on growth and okadaic acid production from the marine dinoflagellate *Prorocentrum belizeanum*. *Toxins* 2014;**6**:229–53.

- Lund-Hansen LC, Hawes I, Sorrell BK, et al. Removal of snow cover inhibits spring growth of Arctic ice algae through physiological and behavioral effects. *Polar Biol* 2014;**37**:471–81.
- McMinn A, Ashworth C, Ryan K. Growth and productivity of Antarctic sea ice algae under PAR and UVR irradiances. *Bot Mar* 1999;**42**:401–7.
- McMinn A, Ryan K, Gademann R. Diurnal changes in photosynthesis of Antarctic fast ice algal communities determined by pulse amplitude modulation fluorometry. *Mar Biol* 2003;**143**:359–67.
- Meiners K, Fehling J, Granskog MA, et al. Abundance, biomass and composition of biota in Baltic Sea ice and underlying water (March 2000). *Polar Biol* 2002;**25**:761–70.
- Menden-Deuer S, Lessard EJ. Carbon to volume relationships for dinoflagellates, diatoms, and other protist plankton. *Limnol Oceanogr* 2000;**45**:569–79.
- Moroz AL, Ehrman JM, Clair TA, et al. The impact of ultraviolet-B radiation on the motility of the freshwater epipelagic diatom *Nitzschia linearis*. *Glob Change Biol* 1999;**5**:191–9.
- Müller A. Photoacclimation of open Baltic algal associations. *Bot Mar* 2004;**47**:2–20.
- Müller S, Uusikivi J, Vähätalo AV, et al. A Bio-optical model for photosynthesis in sea ice. Submitted.
- Niemi M, Kuparinen J, Uusi-Rauva A, et al. Preparation of <sup>14</sup>C-labeled algal samples for liquid scintillation counting. *Hydrobiologia* 1983;**106**:149–56.
- Nilawati J, Greenberg BM, Smith REH. Influence of ultraviolet radiation on growth and photosynthesis of two cold ocean diatoms. *J Phycol* 1997;**33**:215–24.
- Norrman B, Andersson A. Development of ice biota in a temperate sea area (Gulf of Bothnia). *Polar Biol* 1994;**14**:531–7.
- Olenina I, Hajdu S, Edler L, et al. Biovolumes and size-classes of phytoplankton in the Baltic Sea. *Balt Sea Environ Proc* 2006;**106**:1–144.
- Perovich D, Grenfell T, Light B, et al. Seasonal evolution of the albedo of multiyear Arctic sea ice. *J Geophys Res* 2002;**107**:8044.
- Perovich D, Roesler C, Pegau W. Variability in Arctic sea ice optical properties. *J Geophys Res* 1998;**103**:1193–208.
- Petrou K, Hill R, Doblin MA, et al. Photoprotection of sea-ice microalgal communities from the East Antarctic pack ice. *J Phycol* 2011;**47**:77–86.
- Piiparinen J, Enberg S, Rintala J-M, et al. The contribution of MAAs, CDOM and particles to the UV protection of sea-ice organisms in the Baltic Sea. *Photochem Photobiol* 2015;**14**:1025–38.
- Piiparinen J, Kuosa H. Impact of UVA radiation on algae and bacteria in Baltic Sea ice. *Aquat Microb Ecol* 2011;**63**:75–87.
- Piiparinen J, Kuosa H, Rintala J-M. Winter-time ecology in the Bothnian Bay, Baltic Sea: nutrients and algae in fast ice. *Polar Biol* 2010;**33**:1445–61.
- Platt T, Gallegos CL, Harrison WG. Photoinhibition of photosynthesis in natural assemblages of marine phytoplankton. *J Mar Res* 1980;**38**:687–701.
- Richardson K, Beardall J, Raven JA. Adaptation of unicellular algae to irradiance: an analysis of strategies. *New Phytol* 1983;**93**:157–91.
- Rijstenbil JW. Assessment of oxidative stress in the planktonic diatom *Thalassiosira pseudonana* in response to UVA and UVB radiation. *J Plankton Res* 2002;**24**:1277–88.
- Rintala J-M, Piiparinen J, Blomster J, et al. Fast direct melting of brackish sea-ice samples results in biologically more accurate results than slow buffered melting. *Polar Biol* 2014;**37**:1811–22.
- Rintala J-M, Piiparinen J, Ehn J, et al. Changes in phytoplankton biomass and nutrient quantities in sea ice as responses to light/dark manipulations during different phases of the Baltic winter 2003. *Hydrobiologia* 2006;**554**:11–24.
- Rintala J-M, Piiparinen J, Uusikivi J. Drift-ice and under-ice water communities in the Gulf of Bothnia (Baltic Sea). *Polar Biol* 2010;**33**:179–91.
- Ryan KG, McMinn A, Hegseth EN, et al. The effects of ultraviolet-B radiation on Antarctic sea-ice algae. *J Phycol* 2012;**48**:74–84.
- Ryan KG, McMinn A, Mitchell KA, et al. Mycosporine-like amino acids in Antarctic sea ice algae, and their response to UVB radiation. *Z Naturforsch* 2002;**57C**:471–7.
- Salonen K. Rapid and precise determination of total inorganic carbon and some gases in aqueous solutions. *Water Res* 1981;**15**:403–6.
- Santas R, Santas P, Lianou C, et al. Community responses to UVR radiation. II. Effects of solar UVB on field-grown diatom assemblages of the Caribbean. *Mar Biol* 1998;**131**:163–71.
- Steemann Nielsen E. The use of radioactive carbon (<sup>14</sup>C) for measuring organic production in the sea. *J Cons Int Explor Mer* 1952;**18**:117–40.
- Ütermöhl H. Zur Vervollkommnung der quantitativen Phytoplankton-Methodik. *Mitt Int Ver Limnol* 1958;**9**:1–38.
- Uusikivi J, Vähätalo AV, Granskog MA, et al. Contribution of mycosporine-like amino acids and colored dissolved and particulate matter to sea ice optical properties and ultraviolet attenuation. *Limnol Oceanogr* 2010;**55**:703–13.
- Villafañe V, Helbling EW, Holm-Hansen O, et al. Acclimatization of Antarctic natural phytoplankton assemblages when exposed to solar ultraviolet radiation. *J Plankton Res* 1995;**17**:2295–306.
- Wang Q, Hou Y, Miao J, et al. Effect of UVR-B radiation on the growth and antioxidant enzymes of Antarctic sea ice microalgae *Chlamydomonas* sp. ICE-L. *Acta Physiol Plant* 2009;**31**:1097–102.
- Wangberg SA, Persson A, Karlson B. Effects of UV-B radiation on synthesis of mycosporine-like amino acid and growth in *Heterocapsa triquetra* (Dinophyceae). *J Photochem Photobiol B* 1997;**37**:141–6.
- Williamson CE, Salm C, Cooke SL, et al. How do UVR radiation, temperature, and zooplankton influence the dynamics of alpine phytoplankton communities? *Hydrobiologia* 2010;**648**:73–81.
- Wulff A, Wängberg S-Å, Sundbäck K, et al. Effects of UVB radiation on a marine microphytobenthic community growing on a sand-substratum under different nutrient condition. *Limnol Oceanogr* 2000;**45**:1144–52.